Clavulanic Acid Degradation in Streptomyces clavuligerus Fed-Batch Cultivations

ARTICLE *in* BIOTECHNOLOGY PROGRESS · DECEMBER 2001

Impact Factor: 2.15 · DOI: 10.1021/bp020294n · Source: PubMed

5 AUTHORS, INCLUDING:

Hans Roubos
Royal DSM
80 PUBLICATIONS **2,693** CITATIONS
SEE PROFILE

Wim de laat
wim de laat consultancy b.v.
7 PUBLICATIONS **461** CITATIONS
SEE PROFILE

Robert Babuska
Delft University of Technology
330 PUBLICATIONS **5,619** CITATIONS
SEE PROFILE

Clavulanic Acid Degradation in *Streptomyces clavuligerus* Fed-Batch Cultivations

Johannes A. Roubos,*,†,‡ Preben Krabben,‡ Wim T. A. M. de Laat,§ Robert Babuška,† and Joseph J. Heijnen‡

Control Systems Engineering, Faculty of Information Technology and Systems, Delft University of Technology, P.O. Box 5031, 2600 GA Delft, The Netherlands, Kluyver Laboratory for Biotechnology, Faculty of Applied Sciences, Delft University of Technology, Julianalaan 67, 2628 BC Delft, The Netherlands, and DSM Anti-Infectives, P.O. Box 1, 2600 MA, Delft, The Netherlands

Clavulanic acid (CA) is an important antibiotic that is produced by *Streptomyces clavuligerus*. CA is unstable and product degradation has turned out to have a major impact on product titers in fed-batch cultivations. Three different types of experiments have been used to elucidate CA degradation under fed-batch cultivation conditions. First, the influence of individual medium compounds was examined. Second, degradation was monitored during the exponential growth phase in batch cultivations. Third, CA degradation was studied in the supernatant of samples taken during a fed-batch. In addition, data from six fed-batch cultivations were studied to derive information about CA degradation during the production phase. These cultivations were based on a mineral medium, containing glycerol, glutamate, ammonium, and phosphate as the main nutrients. The ammonium concentration had a large influence on the degradation rate constant. In addition, either changes in the substrate availability or high concentrations of ammonium or glycerol cause a major increase in the degradation rate constant. Finally, a linear and a fuzzy logic model were made to predict CA degradation rates in these fed-batches.

1. Introduction

Clavulanic acid (CA) is produced by *Streptomyces clavuligerus* and is a potent β-lactamase inhibitor that has been successfully applied in combination with β-lactam antibiotics, e.g., amoxicillin and ticarcillin disodium. *Streptomyces clavuligerus* is usually cultivated on complex media; however, some studies for mineral media are available. CA is produced when phosphate or nitrogen are at growth-limiting concentrations (*1*). At high growth rates (>0.10 h^{-1}) no CA is produced, whereas at low growth rates (<0.05 h^{-1}) simultaneous growth and product formation takes place (*2*). Product titers of 300−1000 mg/L have been reported for both batch and fed-batch cultures on mineral and complex media (*3*).

Crude CA is unstable (*4*, *5*) and product degradation has a major effect on product titers in fed-batch cultivations. However, only one study about CA decomposition in relation to the production process has appeared in the literature (*2*). Several other works dealt with the stability of CA in aquaous solutions (*5*), stability in the human body (*6*), or with degradation products (*7*, *8*).

Haginaka et al. (*5*) studied CA stability in buffered aqueous solutions at various pH's at 35 °C and ionic strength of 0.5. Degradation follows pseudo-first-order kinetics and is severely affected by catalysis due to buffer salts (citrate, acetate, phosphate, borate, and carbonate). The degradation rate constant k_d is highly dependent on the pH, i.e., a logarithmic plot of k_d vs pH is parabolic with a minimum at pH 6.4 and a steep slope toward acidic or basic conditions (*2*, *5*). CA is about 10 times less stable than penicillin G at neutral pH, five times less stable in the alkaline region and similar in the acidic region. Furthermore, a linear relation between k_d and the phosphate concentration was found for a pH between 5 and 8. In addition, temperature has a major effect on CA degradation (*2*, *5*).

Mayer and Deckwer (*2*) described simultaneous production and decomposition in a laboratory fed-batch process with *S. clavuligerus* on complex medium containing either soy bean extract or soy bean particles. Significant differences between both media were observed for growth, product formation, and degradation in fed-batch cultivations at 27 °C and pH 6.5. The observed degradation rate constants were in the range 0.005−0.040 h^{-1}. The in vivo decomposition rates at 27 °C were 2- to 10-fold higher than in vitro observed degradation rate constants at 21 °C in sterilized samples.

In our previous fed-batch experiments (*9*) significant product degradation was observed. CA degradation is therefore an important aspect to study when optimizing the CA production process. In contrast to (*2*), we study CA degradation in mineral fed-batch media and focus on quantification of the degradation rate. First, in vitro degradation experiments are performed to quantify the effect of the individual medium components. Thereafter, in vivo degradation is studied during growth in batch experiments and during a fed-batch experiment, in both the cultivation broth and the supernatant. Finally, a

* To whom correspondence should be addressed. Phone: +31 15 2783371. E-mail: hans@ieee.org.

† Control Systems Engineering, Faculty of Information Technology and Systems.

‡ Kluyver Laboratory for Biotechnology, Faculty of Applied Sciences.

§ DSM Anti-Infectives.

10.1021/bp020294n CCC: $22.00
Published on Web 00/00/0000

linear model and a nonlinear fuzzy logic model are developed for the degradation rate constant based on data from six fed-batch cultivations. These models may be applied as part of a complete process model that can be applied for process optimization.

2. Materials and Methods

Three different types of experiments have been performed to study CA degradation under fed-batch cultivation conditions. First, the influence of individual medium compounds was examined. Second, degradation was monitored during the exponential growth phase in batch cultivations. Third, CA degradation was studied in the supernatant of samples taken during a fed-batch experiment. Experimental details of three batch and six fed-batch cultures are provided in this section. Additional details about the individual CA degradation experiments are given in the corresponding subsections.

2.1. Strain, Media, and Culture Conditions. One milliliter of *S. clavuligerus* CBS 226.75 mycelia, stored in 80% glycerol at −80 °C, was revived and precultivated in a 250-mL shake flask with one baffle and 50 mL of medium. The cells were grown for 26 h in a shaker incubator at 220 rpm at 28 °C in a medium containing 15 g/L glycerol, 15 g/L soy peptone, 3.0 g/L sodium chloride, and 1.0 g/L calcium carbonate and an initial pH of 6.8. The revived culture was inoculated at 10% v/v into a chemically defined medium identical to the subsequent bioreactor medium. This step was carried out in 2-L shake flasks without baffles containing 500 mL of broth. The pH was buffered by 10.5 g/L MOPS. After 20 h of cultivation, 1 L of preculture was inoculated into a 42-L Applikon bioreactor containing 25 L of medium or into a 20-L Applikon bioreactor containing 14 L of medium. The medium for the fed-batches was designed to yield 5 g DW/L biomass in the growth phase, which ends by phosphate depletion. The medium composition was glycerol 9.3 g/L, K_2HPO_4 0.58 g/L, $(NH_4)_2SO_4$ 1.26 g/L, monosodium glutamate 9.8 g/L, $FeSO_4 \cdot 7H_2O$ 0.18 g/L, $MgSO_4 \cdot 7H_2O$ 0.72 g/L, basildon antifoam 0.09 g/L, and 1.44 g/L of trace elements solution. The composition of the trace element solution contained H_2SO_4 (96%) 20.4 g/L, citrate$\cdot 1H_2O$ 50 g/L, $ZnSO_4 \cdot 7H_2O$ 16.75 g/L, $CuSO_4 \cdot 5H_2O$ 2.5 g/L, $MnCl_2 \cdot 4H_2O$ 1.5 g/L, H_3BO_3 2 g/L, and $NaMoO_4 \cdot 2H_2O$ 2 g/L. The medium for the three batch experiments contained double amounts of glycerol, glutamate, ammonium, and phosphate.

2.2. Cultivations. Six fed-batch experiments (FB3−FB7, FB9) were performed in a 42-L Applikon bioreactor and three batch experiments (B13−B15) in a 20-L Applikon bioreactor. Both were equipped with two 6-bladed Rushton turbines. The temperature was controlled at 30 °C and the pH at 7.0 with 4 N H_2SO_4 and 4 N NaOH as the pH regulators, except for FB7 and FB9, where NH_4OH 3.5 mol/L was used for pH control. The dissolved oxygen concentration was controlled at 50% air saturation by the stirrer rate. The foam level was controlled by adding antifoam (Basildon silicone antifoam, Basildon Chemicals Ltd, U.K.). Mass flows could be followed on-line as the fermentor and bottles with acid, base, and antifoam, as well as the feed media, had been placed on electronic balances. Oxygen and carbon dioxide concentrations were measured on-line by, respectively, a Beckman 864 infrared detector (Rosemount Analytics, USA) and a Servomex 1100A oxygen analyzer (Taylor Servomex Co., USA). The ingoing gas flow (mol/min) was set point controlled by a mass flow controller. The outgoing flow was calculated from the N_2 gas balance. Samples of 100 mL were taken regularly with time intervals of 4−8 h. During feeding in the fed-batch, larger samples were taken to keep the broth volume approximately at a constant level of about 26−28 L. Biomass dry weight was measured in duplicate by centrifugation of 10 mL of broth at 3000*g* for 2 × 10 min followed by washing with demineralized water and centrifugation. The test tubes were dried for at least 24 h at 105 °C. Glycerol was separated on a BioRad HPX-87H 300 × 7.8 mm column equipped with a BioRad cation-H refill cartridge 30 × 4.6 mm precolumn. The eluent was 1.5 mM phosphoric acid with 0.6 mL/min flow. Glycerol was detected by refractive index. Clavulanic acid was determined spectophotometrically by reaction with imidazole (*10*). Glutamate was determined enzymatically by use of glutamate dehydrogenase/diaphorase coupled assay (*11*). Ammonium was measured on an autoanalyzer (Skalar, Breda, The Netherlands) based on a modified Berthelot reaction (*12*). Phosphate was measured spectrophotometrically by the ascorbic acid method (*13*).

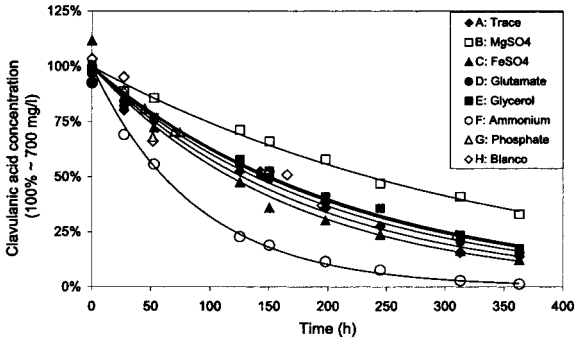

Figure 1. Experimental results for CA degradation experiments, as described in Table 1.

Table 1. Components in the Shake Flasks and CA Degradation

	medium components	k_d (h^{-1})
A	trace elements (1.6 mL/L), MOPS, CA	0.0054
B	$MgSO_4 \cdot 7H_2O$ (0.8 g/L), MOPS, CA	0.0029
C	$FeSO_4 \cdot 7H_2O$ (0.2 g/L), MOPS, CA	0.0059
D	glutamate (21.8 g/L), MOPS, CA	0.0050
E	glycerol (20.6 g/L), MOPS, CA	0.0046
F	$(NH_4)_2SO_4$ (2.8 g/L), MOPS, CA	0.0114
G	phosphate (1.2 g/L K_2HPO_4), MOPS, CA	0.0047
H	MOPS, CA	0.0047

3. Clavulanic Acid Degradation Experiments

3.1. Influence of Medium Components on CA Degradation. ***Experiment Design.*** The in vitro influence of individual medium components on clavulanic acid were studied in shake flasks. Shake flasks of 500 mL with one baffle were filled with 50 mL of different combinations of medium components as described in Table 1 and heat-sterilized. About 30 mg of CA was added through a sterile filter. The shake flasks were maintained at 30 °C and stirred at 200 rpm, and degradation was followed. The initial pH was maintained at 7.0 by 10.5 g/L MOPS buffer.

Results. The degradation rate followed first-order kinetics, and degradation rate constants were estimated (Table 1). The measured data, normalized by an estimate for the initial CA concentration, are plotted in Figure 1, where 100% is 700 ± 100 mg/L. Ammonium strongly increases the degradation rate constant, whereas magnesium reduces the degradation rate constant. No effect of trace elements, iron, glutamate, glycerol, or phosphate was observed.

Table 2. CA Degradation during the Exponential Growth Phase

	stirrer rate (rpm)	μ from CER (h^{-1})	μ from acid addition (h^{-1})	k_d (h^{-1})
B13	350	0.104	0.101	0.0100
B14	763	0.109	0.111	0.0116
B15	763	0.126	0.130	0.0109

3.2. CA Degradation in the Batch Growth Phase. ***Experiment Design.*** CA was added to the medium in three batch cultivations (B13−B15). These cultivations were inoculated with 1 L of preculture and 14 L of medium. About 1300 mg/L CA was added to the medium, and degradation was followed during the cultivation at pH 7.0 and 30 °C. Low and high stirrer rates were applied to study their effect on biomass formation and cell lysis; i.e., in previous batch experiments, the DO was controlled above 50% by the stirrer rate and large amounts of cell lysis were observed at high stirrer rates during exponential growth (*14*).

Results. CA production is considered zero during exponential growth because the growth rate is high and only marginal production was observed in previous experiments and the fed-batch experiments described in this paper. Degradation rate constants were derived from CA profiles and are summarized in Table 2. This table also provides the estimated maximum specific growth rates, based on the continuously monitored carbon dioxide evolution rate (CER) (mol CO_2/kg h^{-1}) and acid addition rate (mol H^+ h^{-1}). Data from 10 h after inoculation till the end of the growth phase were used to estimate specific growth rates, i.e., constant specific growth rates were observed till the growth phases ended as a result of phosphate depletion between 31 and 35 h after inoculation. The degradation rate constant during the growth phase was around 0.011 h^{-1}. This value is similar to the one obtained for CA degradation in sample F in Section 3.1, containing a similar concentration of ammonium. This means that biomass has no additional effect on the CA degradation rate constant; biomass was measured at 26 h and was 7 ± 1 g DW/L for B13−B15)].

It is remarkable that the specific growth rate was much lower than in previous batch experiments without CA in the medium and specific growth rates of 0.18 ± 0.01 h^{-1} (*14*). Moreover, a lower growth rate was expected at the high stirrer speeds, where cell lysis was expected (*14*). Both observations indicate severe inhibition of growth by CA. A change in cell wall composition or cell size may explain the fact that less lysis was observed at the high growth rates.

3.3. CA Degradation in a Fed-Batch. ***Experiment Design.*** Six large samples of about 400 mL were taken during fed-batch cultivation FB9 (indicated in Figure 2a). These samples were spun down at 13 000*g* for 5 min. The supernatant was separated from the pellet, and approximately ∼25 mg of CA was added to ∼25 mL of the supernatant. The CA degradation was followed over time at 20, 25, and 30 °C in closed bottles. In addition, part of the supernatant of two samples was heat-sterilized at 121 °C for 20 min, and ∼25 mg of CA was added to ∼25 mL of sterilized supernatant. CA degradation was followed over time at 30 °C in closed bottles.

Fed-Batch FB9. FB9 was started with a batch growth phase on glycerol, glutamate, ammonium, and phosphate designed to yield 5 g/L DW biomass. Growth stopped after phosphate was depleted and then CA production was induced. Five hours later, a constant feed with glycerol and a growth-limiting amount of phosphate was started. In addition, ammonium was used for pH regulation. The

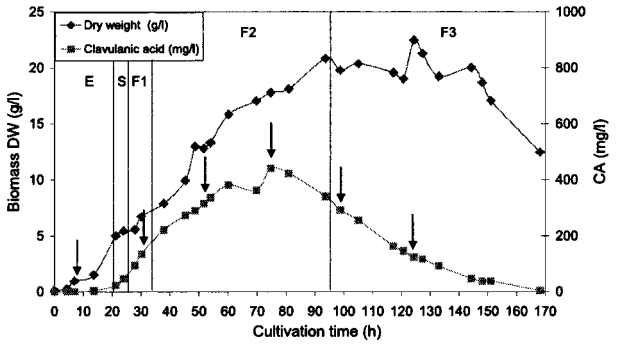

(a) Biomass and CA

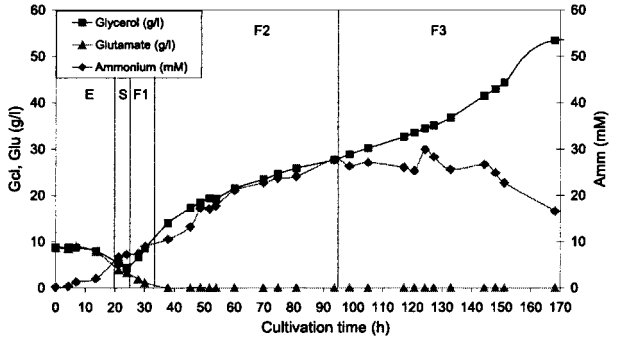

(b) Glutamate, glycerol and ammonium

Figure 2. Data from fed-batch FB9. The arrows in indicate samples used to study CA degradation in the supernatant.

measured concentration profiles of biomass and CA are shown in Figure 2a and those of glycerol, glutamate, and ammonium in Figure 2b. The broth volume was kept around 27 L by taking samples. In our analysis, five phases are distinguished (E = exponential growth, S = stationary, F = feed):

- E: exponential growth; phase ends at 20 h as a result of phosphate depletion;
- S: stationary phase without phosphate; CA formation is induced;
- F1: constant feeding; growth on glycerol, glutamate, ammonium, and phosphate; growth phase ends at 32 h with glutamate depletion;
- F2: constant feeding; growth on glycerol, ammonium and phosphate; around 70 h, CA production stops for unknown reasons;
- F3: at 94 h, a change in air-flow rate severely affects cell growth; finally cells start dying at 140 h.

Carbon and nitrogen balances were made; however, these only fitted for the exponential growth phase. The gap in these balances is mainly due to cell lysis caused by mechanical stress, as was shown in ref 14. Cell lysis in the feed phase was described in ref 9 as a percentage of the growth rate, estimated to be 25% for FB9. The maximum biomass level was 21 g DW/L. At 94 h, the air-flow was changed from 10 to 20 L/h and the air filter was changed. This resulted in an acid pulse due to changes in the CO_2/H_2CO_3 equilibrium, and the DO became close to 0 for a short moment. Biomass growth was severely damaged after this occurrence. The concentration and the amount of biomass is approximately constant in feeding phase F3 between 94 and 145 h, i.e., simultaneous growth and cell lysis occur. The maximum CA level was 430 mg/L, but only 20 mg/L was left at the end of the fed-batch.

Results. CA degradation rate constants in the supernatant of the FB9 samples at 20, 25, and 30 °C are shown

Table 3. CA Degradation Rate Constants in the Fed-Batch Cultivations[a]

fed-batch no.	Gcl feed (g/kg h^{-1})	Glu feed (g/kg h^{-1})	Amm feed (mmol/kg h^{-1})	Phos feed (mg/kg h^{-1})	k_d (h^{-1})	cultivation time (h)
FB3	0.6		1.0	2.3	0.004	120−145
	1.2		1.0	2.3	0.010	145−190
FB4	0.9	0.3	0.4	4.5	0.004	80−105
	0.9	0.3	0.4	4.5	0.016	105−145
FB5	1.2	0.3	0.4	4.5	0.005	100−120
					0.010	120−150
FB6	0.9	0.3		4.5	0.004	80−110
		0.3		4.5	0.015	110−145
FB7	0.6		1.0−2.0[b]	3.0	0.009	120−170
FB9	1.2		1.0−1.5[b]	3.0	0.020	80−105
	1.2		1.0−1.5[b]	3.0	0.035	105−160

[a] The feed rates are approximate ones since the fed-batch volume is 27 ± 3 kg and varies in time, and the cultivation time is the time at which k_d is estimated. [b] In FB7 and FB9, ammonium feed is determined by pH control, therefore it depends on biomass concentration and specific substrate uptake rates. An estimated feed range is given.

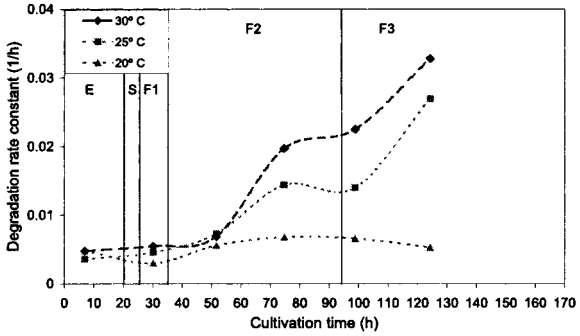

Figure 3. CA degradation constant for the FB9 samples at 20, 25, and 30 °C.

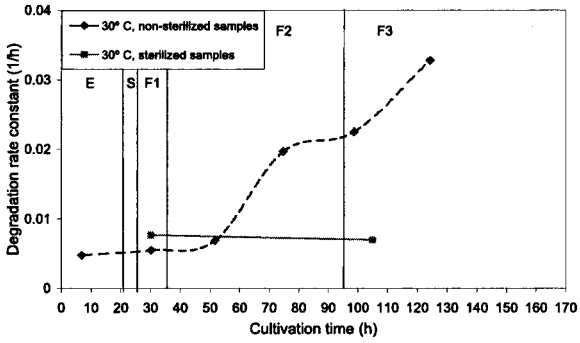

Figure 4. CA degradation in supernatant (nonsterilized) and in heat-sterilized supernatant of FB9 samples at 30 °C.

in Figure 3. Early in the cultivation, k_d is approximately 0.005 h^{-1}. This is in agreement with the in vitro experiment, considering the ammonium level is more than twice as low, i.e., <20 mM, while it is 42 mM in Section 3.1. The degradation rate constant increases during the cultivation time, and a much higher k_d occurs around 70 h. The exact moment cannot be derived from Figure 3, but from Figure 2a is clear that the increase in product concentration declines after 60 h. CA production completely stopped after 74 h, and k_d increased 4-fold to 0.020 h^{-1}. An induced enzyme or a chemical compound may have caused this increase. It is not likely that this was caused by a commonly present intracellular enzyme, because substantial cell lysis already occurred after 25 h of cultivation. Additional evidence for enzymatic degradation was obtained in a degradation experiment with two sterilized samples of FB9, as shown in Figure 4. After 74 h, k_d was sensitive to pretreatment by heat sterilization, while samples before were not. This indicates that the high k_d was partly caused by enzymatic reactions or catalyzed by heat-sensitive components. In phase F3, k_d

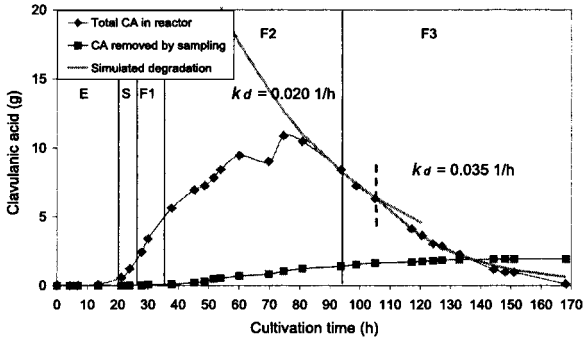

Figure 5. Estimation of CA degradation from FB9 data; k_d is initially 0.020 h^{-1} and increases around 110 h, as indicated by the dashed line, to 0.035 h^{-1}.

increased even further to 0.035 h^{-1}. This is possibly caused by a change in metabolism or high amounts of cell lysis.

In phases without CA production, k_d values can be estimated directly from the fed-batch data under the assumption that k_d is approximately constant for a certain part of the cultivation time; i.e., the real k_d is not constant but depends on substrate concentrations and other factors that change during a fed-batch cultivations. However, if conditions do not change a lot, a reasonable approximation can be obtained as will be shown. For example, in FB9, production can be assumed to be zero after 74 h and k_d is about 0.020 h^{-1} at the end of F2 and 0.035 h^{-1} in F3 (Figure 5). These values were obtained by manually tuning a simulation of the CA degradation. The simulation is started with the total amount of CA that was present in the fermentor when CA production stopped. CA degrades at a rate k_d, and some of it is removed by taking samples. The k_d values determined in the supernatant of the FB9 samples are similar to the in vivo estimated degradation rate constants in the fermentor. This shows that biomass has no direct influence on the degradation rate constant.

4. CA Degradation Models

In this section, two models will be developed to predict k_d as a function of fermentation conditions. Data from fed-batch cultivations FB3−FB7 and FB9 are used to make a linear and a fuzzy logic model and both are compared.

4.1. Fed-Batch Data. Fed-batch FB3−FB7 and FB9 were started with the same batch medium containing glycerol, glutamate, ammonium, and phosphate (Section *2*). Different feeding compositions were applied (Table 3) and fed at a constant rate. Also, ammonium was applied

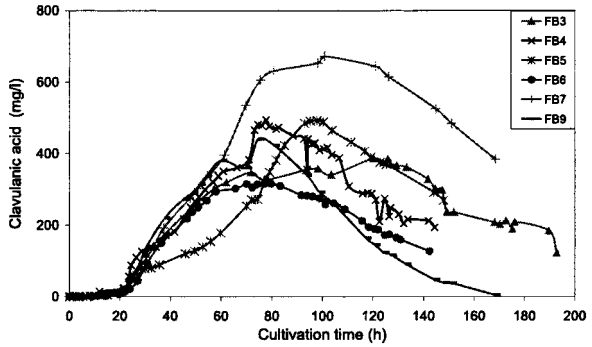

Figure 6. CA profiles for FB3−FB7 and FB9.

for pH regulation in FB7 and FB9. The exponential growth rate was 0.18 h^{-1} until phosphate was depleted after 20 h. Subsequently, feeding was started after a 5 h stationary phase where CA production was induced. The CA concentration profiles are given in Figure 6. Observed degradation rate constants were estimated in a similar way as in Section 3.3 and are given in Table 3.

CA production generally proceeds for about 30−60 h and then stops. Here, k_d is estimated at around 0.004 h^{-1} for FB3−FB6 and stay at this level for about 30−70 h. This k_d is 2−2.5 times lower than that during growth in the batch experiments (Table 1), which can be explained by the lower substrate concentrations when the fed-batch cultivations proceed. Thereafter, k_d increases, and possible causes are given. In FB3 it seems related to a quick increase of the glycerol concentration to 180 mM, caused by a manual change in the glycerol feed rate at 124 h, i.e., the glycerol concentration was around 60 mM for about 80 h before this change. In FB4, the k_d increase is related to a short ammonium limitation that occurred. Phosphate and ammonia were fed with a certain ratio based on previous experience; however, the phosphate content of the biomass was greatly reduced under P-limited growth (*9*). This resulted in ammonia depletion, followed by a change in nitrogen metabolism, i.e., ammonia starts accumulating. In FB5, k_d changed after the feeding was stopped, and in FB6, the k_d changed after the glycerol feed stopped. Degradation rate constants in FB7 and FB9 were high directly after CA production stopped. In FB7, this high k_d may be related to the high glycerol level (>7 g/L) and ammonium level (>15 mM) that occur. In FB9 it may also be related to the highly increased glycerol level (>25 g/L). A second increase occurs at an increasing ammonium level (>15 mM).

Concluding, k_d increases when metabolism is affected by a change in substrate availability. In addition, high ammonium or glycerol concentrations seem to increase k_d highly, i.e., in FB7 and FB9, high ammonium and/or glycerol levels may have induced a CA degrading enzyme, as discussed in Section 3.3.

4.2. Model Identification and Tuning. On the basis of the available data, a linear model and a fuzzy logic rule-based model (*15*) are made to predict the clavulanic acid degradation rate. The fuzzy logic model is a rule-based model of the Takagi−Sugeno type (*16*). This is a local linear modeling approach where rules define the operating region of the models. The rules consist of conditions that are specified by means of membership functions in [0, 1] which are the fuzzy sets. Several data-based identification techniques exist to derive TS-fuzzy models.

First, an initial linear and fuzzy model are identified based on k_d estimates given in Table 3. Both models are suboptimal because the used k_d values were *roughly* estimated from the fed-batch data and not the *real* ones. Therefore, both model are tuned by applying a simulation method. The difference between the model simulation and smoothed real output, measured as a weighted mean squared error (WMSE), is used as the objective function to be minimized, i.e., MSE values were calculated for each fed-batch, then summed up and divided by the number of fed-batches. A real-coded genetic algorithm is applied to optimization by allowing certain variations around the parameters of the initial model. Details of the applied model-tuning technique are explained in ref 17. The GA population-size contained 20 individuals from which 10 individuals were replaced in each generation, with a 20% mutation and a 80% crossover ratio for 200 generations.

4.3. Results. Concentration profiles of FB3−FB7 and FB9 are resampled at 1-h intervals and smoothed by a zero-phase forward-backward filter. Biomass (g/L), glycerol (g/L), glutamate (g/L), ammonium (mM), CA (mg/L), and growth (positive, zero, negative) are considered as model inputs. Correlation between smoothed concentration profiles, type of growth, and the estimated k_d values in Table 3 was calculated. Glycerol and ammonium correlate highly positive with k_d, CA has a negative correlation, and biomass, growth, and glutamate did not show any correlation. Phosphate was left out because it was assumed zero in the applied fed batches, but also no P-effect was observed in the medium component degradation experiments. Note that only those parts of the fed-batches are used for which it is assumed that CA production has stopped. In addition, data from the degradation in medium (Section 3.1) are used and weighted 20% with the fed-batch data during model optimization. The best (initial) models were obtained when using the glycerol concentration (*gcl*) in (g/L) and ammonium concentration (*amm*) in (mM) as model inputs, when considering also the number of inputs in relation to the small numbers of data that are available.

Linear Model. The initial linear model was obtained from least-squares estimation, using smoothed fermentation data and k_d estimates from Table 3:

$$\hat{k}_d = (0.49gcl + 0.21amm + 3.18) \times 10^{-3} \qquad (1)$$

In Figure 7a, the prediction surface is shown together with the estimated the estimated k_d values from Table 3. The mean WMSE of this model is 0.028×10^{-3}. Tuning of this model by the simulation and GA, with 50% variation around the initial parameters, resulted in

$$\hat{k}_d = (0.68gcl + 0.22amm + 4.11) \times 10^{-3} \qquad (2)$$

which has a WMSE of 0.018×10^{-3}. Simulations are shown in Figure 8a.

Fuzzy Model. GK clustering was applied to obtain an initial TS-fuzzy model (*18*). Clustering is done for k input-output data pairs $\{x_k, y_k\}$, where $\boldsymbol{x} = [x_1, ..., x_n]^T = [gcl, amm]^T$ is the input vector and $y_k = (k_d)_k$ the output. The following two-rule fuzzy model was obtained, using smoothed fermentation data and k_d estimates from Table 3:

R_1: **If** *gcl* is A_{11} **and** *amm* is A_{21} **then** $\hat{y}_i =$
$$(-0.84gcl + 0.15amm + 4.3) \times 10^{-3}$$

R_2: **If** *gcl* is A_{12} **and** *amm* is A_{22} **then** $\hat{y}_i =$
$$(0.46gcl + 0.73amm + 5.8) \times 10^{-3}$$

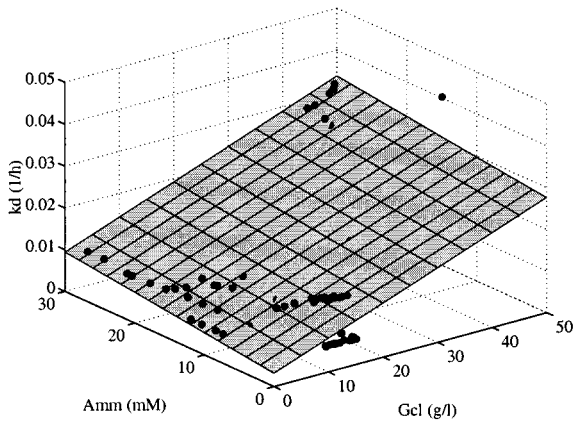

(a) Linear model

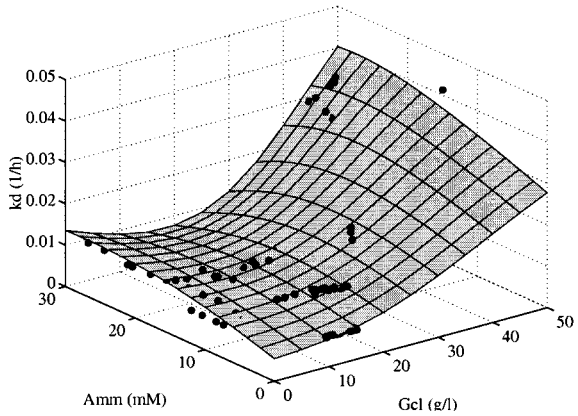

(b) Two-rule fuzzy model

Figure 7. Model predictions for degradation rate constants (data are partly below the surface).

where $\hat{y}_i$ is the output of the ith rule, and A_{i1}, ..., A_{in} are fuzzy sets defined in the antecedent space by membership functions $\mu_{A_{ij}}(x_j)$:$\mathbb{R} \rightarrow [0, 1]$, shown in Figure 9. The fuzzy model output k_d, is computed by aggregating the individual contributions of the M rules:

$$\hat{k}_d = \sum_{i=1}^{M} p_i(\boldsymbol{x})\hat{y}_i \tag{3}$$

where $p_i(\boldsymbol{x})$ is the normalized firing strength of the ith rule:

$$p_i(\boldsymbol{x}) = \frac{\prod_{j=1}^{n} A_{ij}(x_j)}{\sum_{i=1}^{M}\prod_{j=1}^{n} A_{ij}(x_j)}, \quad i = 1, 2, \ldots, M. \tag{4}$$

In Figure 7b, the prediction surface is shown together with the estimated k_d values from Table 3. The mean square error (WMSE) for simulation is 0.018×10^{-3}. Next, the membership function A_{12} for glycerol was removed because it is similar to the universal set. Tuning of this model by the simulation and GA, with 20% variation around the initial parameters, resulted in a model with WMSE $= 0.007 \times 10^{-3}$. Simulation results are shown in Figure 8b and the optimized membership functions are shown in Figure 9. These can be labeled as "Low" and "High". The following rules, for a low and a high ammonium concentration, are obtained:

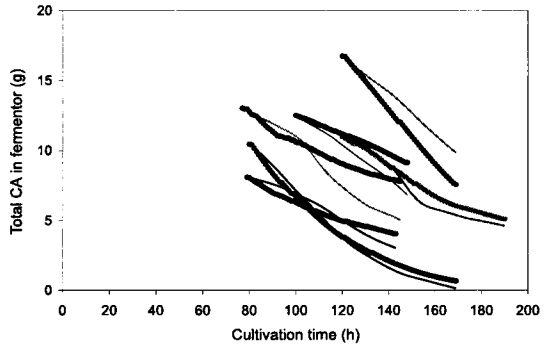

(a) Linear model

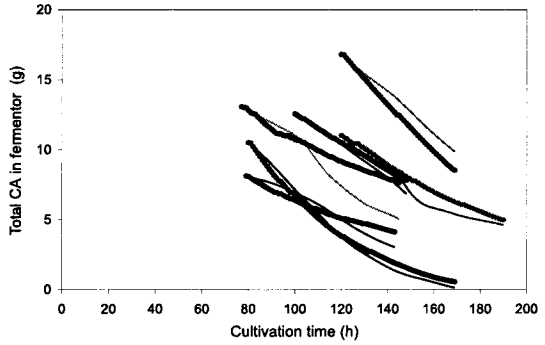

(b) Two-rule fuzzy model

Figure 8. Simulation of the tuned model (thick lines) plotted together with the smoothed data of FB3−FB7 and FB9 (thin lines).

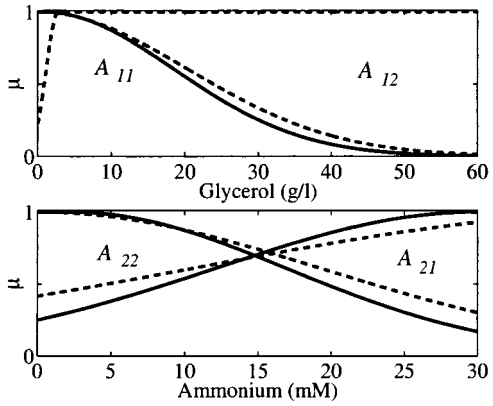

Figure 9. Membership function of the initial model (dashed) and final model (line).

R_1: **If** *gcl* is Low ***and*** *amm* is High **then** $\hat{y}_i =$
$$(-0.63gcl + 0.20amm + 4.4) \times 10^{-3}$$

R_2: **If** *amm* is Low **then** $\hat{y}_i =$
$$(0.72gcl + 0.63amm + 6.2) \times 10^{-3}$$

The fuzzy model is superior to the linear model, because it described the different behaviors of k_d at low and high glycerol concentrations.

5. Discussion

In the in vitro degradation experiments, ammonium and magnesium were the only two compounds that had a big influence on k_d. Glycerol had no influence, although it seems to have influence in the fed-batch experiments. Indications for a metabolic reaction and the occurrence of a CA degrading enzyme at high glycerol levels late in the cultivation were found by comparing sterilized and

nonsterilized samples in FB9. Unfortunately, detection of β-lactamase activity by a spectrophotometric method with nitroficin was not possible because of medium interference. In addition, a reduced k_d was observed at lower temperatures, which was known from the literature.

Next, data from six fed-batches was applied to develop a quantitative model for k_d. Good models were obtained as a function of glycerol and ammonium concentration. The fuzzy rule-based model also predicted an effect of high glycerol concentrations on k_d. On the other hand, it is clear that these models cannot explain all the complex behavior leading to increasing degradation rates due to metabolic changes, etc. However, both have a certain predictive capacity and can therefore be applied in an overall model for process optimization.

Concluding, possible ways to reduce the negative CA degradation effect in the fed-batch production are

(i) Optimization of medium and substrate feed profiles such that clavulanic acid is produced at low ammonium and glycerol concentrations. However, in general, it is not easy to keep substrate concentrations at low levels without the risk of running into substrate depletion, which has harmful effects on CA production (Section 4.1). Therefore it is important to develop dynamic models that quantitatively describe substrate consumption, biomass growth, and product formation during a fed-batch cultivation (*9*). The developed k_d models can then be used as part of a complete process model to be used for model-based process optimization.

(ii) Application of a higher magnesium concentration in the medium, because it stabilizes CA and is a cheap compound. However, its effects on biomass formation, CA production and downstream processing are not yet known.

(iii) Application of a temperature profile, i.e., CA degradation is reduced at lower temperatures, but the specific growth rate is also reduced. Moreover, temperature effects on CA production are not yet known.

(iv) Application of a different feeding strategy that results in a longer growth phase and a shorter production phase, i.e., more biomass will be formed while the specific CA production rate will probably not be affected.

(v) On-line product removal as was studied, for example, in ref 19 for cycloheximide production by *S. griseus*.

6. Conclusion

Clavulanic acid degradation is an important aspect that cannot be neglected when optimizing the fed-batch production process. Medium components, in particular magnesium and ammonium, determine the degradation rate to a certain extent, while at high glycerol and ammonium concentrations probably an enzyme is induced that increases the degradation rate constant. Finally, a linear and a fuzzy logic model were developed to describe the degradation rate in the fed-batch experiments.

Acknowledgment

This research is done as a part of Delft Interfacultary Research Program *Mastering the Molecules in Manufacturing (M3)* and it is in part financed by DSM Anti-Infectives, Delft, The Netherlands. We are grateful to Sebastian Peeters for performing the clavulanic acid degradation experiments.

References and Notes

(1) Ives, P. R.; Bushell, M. E. Manipulation of the physiology of clavulanic acid production in *Streptomyces clavuligerus*. *Microbiology* **1977**, *143*, 3573−3579.

(2) Mayer, A. F.; Deckwer, W.-D. Simultaneous production and decomposition of clavulanic acid during *Streptomyces clavuligerus* cultivations. *Appl. Microbiol. Biotechnol.* **1996**, *45*, 41−46.

(3) Gouveia, E. R.; Baptista-Neto, A.; Azevedo, A. G.; Badino, A. C., Jr.; Hokka, C. O. Improvement of clavulanic acid production by *Streptomyces clavuligerus* in medium containing soybean derivatives. *World J. Microbiol. Biotechnol.* **1999**, *15*, 623−627.

(4) Baggaley, K. H.; Brown, A. G.; Schofield, C. J. Chemistry and biosynthesis of clavulanic acid and other clavams. *Nat. Prod. Rep.* **1997**, *14*(4), 309−333.

(5) Haginaka, J.; Nakagawa, T.; Uno, T. Stability of clavulanic acid in aqueous solutions. *Chem. Pharm. Bull.* **1981**, *29*(11), 3334−3341.

(6) Bolton, G. C.; Allen, G. D.; Davies, B. E.; Filer, C. W.; Jefferey, D. J. The disposition of clavulanic acid in man. *Xenobiotica* **1986**, *16*(9), 853−863.

(7) Finn, M. J.; Harris, M. A.; Hunt, E.; Zomaya, I. I. Studies on the hydrolysis of clavulanic acid. *J. Chem. Soc., Perkin Trans. 1* **1984**, 1345−1349.

(8) Brown, A. G.; Howarth, T. T.; Ponsford, R. J. The chemistry of clavulanic acid: some reactions of esters under neutral, acedic and basic conditions. *Tetrahedron Lett.* **1983**, *24*(26), 2693−2696.

(9) Roubos, J. A.; Krabben, P.; Luiten, R. G. M.; Babuška, R.; Heijnen, J. J. A Semi-Stoichiometric Model for a Streptomyces Fed-Batch Cultivation with Multiple Feeds. In *Computer Applications in Biotechnology 8*; Dochain, D., Perrier, M., Eds.; Quebec City, Canada, June 24−27 2001, pp 299−304.

(10) Bird, A. E.; Bellis, J. M.; Basson, B. C. Spectrophotometric assay of clavulanic acid by reaction with imidazole. *Analyst* **1982**, *107*, 1241−1245.

(11) Beutler, H. O. *Standard Methods for the Examination of Water and Wastewater*, 3rd ed.; Bergmeyer, H., Ed.; Verlag Chemie: Weinham, 1985.

(12) Krom, M. D. Spectrophotometric determination of ammonia: A study of a modified Berthelot reaction using salicylate and dichloroisocyanurate. *The Analyst* **1980**, *105*, 305−316.

(13) *Standard Methods for the Examination of Water and Wastewater*, 13th ed.; Taras, M. J., Greenberg, A. E., Hoak, R. D., Rand, M. C., Eds.; American Public Health Association: New York, 1971.

(14) Roubos, J. A.; Krabben, P.; Luiten, R. G. M.; Verbruggen, H. B.; Heijnen, J. J. A quantitative approach to characterizing cell lysis caused by mechanical agitation of *Streptomyces clavuligerus*. *Biotechnol. Prog.* **2001**, *17*(2), 336−347.

(15) Wang, L.-X. *A Course in Fuzzy Systems and Control*; Prentice Hall: London, 1997.

(16) Takagi, T.; Sugeno, M. Fuzzy identification of systems and its application to modeling and control. *IEEE Trans. Systems, Man Cybernetics* **1985**, *15*, 116−132.

(17) Setnes, M.; Roubos, J. A. GA-fuzzy modeling and classification: complexity and performance. *IEEE Trans. Fuzzy Systems* **2000**, *8*(5), 509−522.

(18) Babuška, R. *Fuzzy Modeling for Control*; Kluwer Academic Publishers: Boston, 1998.

(19) Dykstra, K. H.; Li, X.-M.; Wang, H. Y. Computer modeling of antibiotic fermentation with on-line product removal. *Biotechnol. Bioeng.* **1988**, *32*, 356−362.

Accepted for publication January 14, 2002.

BP020294N